ENVIRONMENTAL RESEARCH
LETTERS

LETTER

Reducing transatlantic flight emissions by fuel-optimised routing

Cathie A Wells[1], Paul D Williams[1], Nancy K Nichols[1,2], Dante Kalise[3] and Ian Poll[4]

[1] University of Reading, Reading, United Kingdom
[2] National Centre for Earth Observation, Leicester, United Kingdom
[3] University of Nottingham, Nottingham, United Kingdom
[4] Poll AeroSciences Ltd, Bedford, United Kingdom

E-mail: c.a.wells@pgr.reading.ac.uk

Keywords: aircraft, aviation, emissions, flight routes, jet stream, route optimisation

OPEN ACCESS

RECEIVED
6 June 2020

REVISED
13 November 2020

ACCEPTED FOR PUBLICATION
27 November 2020

PUBLISHED
26 January 2021

Original Content from this work may be used under the terms of the Creative Commons Attribution 4.0 licence.

Any further distribution of this work must maintain attribution to the author(s) and the title of the work, journal citation and DOI.

Abstract

After decades of limited situational awareness for aircraft flying in the mid-North Atlantic, full satellite coverage will soon be available. This opens up the possibility of altering flight routes to exploit the wind field fully. By considering flights between New York and London, from 1 December, 2019 to 29 February, 2020, it is shown how changes to current practice could significantly reduce fuel use and, hence, greenhouse gas emissions. When airspeed and altitude are constant, the fuel flow rate per unit time is constant and the route with the minimum journey time uses the least fuel. Optimal control theory is used to find these minimum time routes through wind fields from a global atmospheric re-analysis dataset. The total fuel burn and, hence, the emissions (including CO_2) are proportional to the 'air distance' (the product of airspeed and flight time). Minimum-time routes are compared with the actual routes flown through the wind fields. Results show that current flight tracks have air distances that are typically several hundred kilometres longer than the fuel-optimised routes. Potential air distance savings range from 0.7% to 7.8% when flying west and from 0.7% to 16.4% when flying east, depending on airspeed and which of the current daily tracks is used. Thus, substantial reductions in fuel consumption are possible in the short term. This is in contrast to the incremental improvements in fuel-efficiency through technological advances, which are high cost, high risk and take many years to implement.

1. Introduction

As pressure to reduce global greenhouse gas emissions continues to increase (IPCC 2019), aviation must respond at least as ambitiously as the other transport sectors. Currently aviation is responsible for approximately 2.4% of all anthropogenic sources of CO_2 (Graver *et al* 2019, Grewe *et al* 2019, Lee *et al* 2020), but this figure is growing (Ryley *et al* 2020, Grewe *et al* 2017, Graver *et al* 2019). The International Civil Aviation Organisation (ICAO) has already established a policy of improving the fuel efficiency of international flights by 2% annually (ICAO 2016), through improvements to aircraft technology, sustainable fuels and air traffic management (ATM) and operations (ICAO 2019). However, greater savings are needed. Additionally, 192 nations agreed to CORSIA (Carbon Offsetting and Reduction Scheme for International Aviation) in 2016, pledging to use offset schemes to maintain net emissions at the 2020 level (Timperley 2019). CORSIA only provides short term alleviation, as there are difficulties in ensuring that genuine net emissions reduction takes place.

If the global economy fails to decarbonise sufficiently rapidly, there may be significant consequences for aviation from the ensuing climate change. These consequences include increased turbulence as the jet stream becomes more sheared (Williams and Joshi 2013, Williams 2017, Storer *et al* 2017, Lee *et al* 2019, Kim *et al* 2015), modified flight routes and journey times as the prevailing high-altitude winds shift and strengthen (Karnauskas *et al* 2015, Irvine *et al* 2016, Williams 2016, Kim *et al* 2020), and take-off weight restrictions as warmer air reduces lift and thrust on the runway (Coffel and Horton 2015, Gratton *et al* 2020). Therefore, aviation is not only a contributor to climate change, but may also suffer from its adverse effects increasingly in future.

© 2021 The Author(s). Published by IOP Publishing Ltd

Various alternative solutions to offsetting have been suggested, from greater use of synthetic bio-fuels to replacing the entire air transport fleet of approximately 31 000 aircraft (CAPA 2018) with updated models (Monbiot 2006). However, those technologies that have the potential to produce significant reductions in fuel use are high-risk, high-cost and have implementation timescales measured in decades (Jensen *et al* 2015). By contrast, improvements to current operational procedures, such as routing flights more efficiently, have the potential to provide immediate, low-cost, low-risk, significant reductions (Németh *et al* 2018). Fuel saving through more efficient operations would be a benefit to both the airlines through reduced fuel expenditure and to the environment through reduced emissions.

Historically flight routes across the North Atlantic have been constrained by the large volume of air traffic and the absence of radar coverage in mid-ocean (Dhief 2018). However, a new network of low Earth orbit satellites being tested currently will improve situational awareness dramatically (Aireon 2020). With aircraft able to transmit and receive accurate information continuously, it is now possible to consider the implementation of fuel-optimised routes (NATS 2019). These new routes would take greater advantage of the prevailing eastward winds when flying east and reduce the negative impact of these same air currents when flying west. Air distance, the distance flown by an aircraft relative to the surrounding air, will be used in this study as a measure of the efficiency of a flight path. Ground distance, in contrast, is not related to fuel burn in a simple way, because of the conveyor effect of the winds. As fuel burn is directly proportional to air distance and as emissions, including carbon dioxide, are directly proportional to fuel burn (Henderson *et al* 2012, Green 2009), any saving made in air distance is a valuable step towards meeting the ICAO target.

Currently flight tracks in the North Atlantic's organised track system (OTS) are created on a daily basis by air navigation service providers (ANSPs), NATS in the United Kingdom of Great Britain and Northern Ireland for the westbound paths and NAV CANADA for those going east. These are based primarily on the need to separate aircraft safely, whilst taking some account of the winds. Airlines request their preferred tracks by submitting preferred route messages in the hours before a flight and the ANSPs create a daily track system that reflects the airlines' wishes as closely as possible. An example of these tracks can be seen in figure 1. By calculating the air distances for these ATM tracks and comparing them with the optimised minimum values, the potential savings can be assessed. These savings are characteristic of the route flown and not of the aircraft being used.

Recent research has focused on limiting energy output, rather than time (Franco and Rivas 2011, Burrows 1983, Pierson and Ong 1989, Murrieta Mendoza *et al* 2020). Other strands of route optimisation have considered turbulence avoidance (Jardin and Bryson 2012, Kim *et al* 2015) and balancing the reduction of climate effects with time of flight (Grewe *et al* 2019, 2017). This paper, however, is the first to identify fuel and emissions savings for transatlantic traffic by calculating the excess air distance flown along the current OTS relative to the minimum air distance route. Thus the focus of this paper is CO_2 reduction. Fuel optimised routes are not necessarily climate optimised (Grobler *et al* 2019), as additional effects such as contrail formation, documented in other sources (Teoh *et al* 2020, Poll and Schumann 2020), are not taken into account.

This paper is set out in five sections. In section 2, the different datasets are described. Section 3 explains the analysis method, shows how time optimisation impacts fuel use, how time optimised routes are found and how to compare these with the current tracks. Results showing potential air distance savings across the 91 day trial period are set out in section 4. Finally, the results are summarised and discussed in section 5.

2. Data sources

Flights between London Heathrow Airport (LHR: 51.5°N, 0.5°W) and John F. Kennedy Airport (JFK: 40.6°N, 73.8°W) in New York are modelled both eastbound and westbound. Although the trajectory prediction methods used by airlines are commercially sensitive (Cheung 2018), the resulting tracks are in the public domain. Past flight tracks were downloaded from the https://blackswan.ch/northatlantictracks website, which provides archived eastbound and westbound way points for all paths flown over the last year. Westbound tracks use labels from A to K, where A is always the northernmost route and eastbound tracks are labelled from N to Z with Z being the southernmost route. There are different numbers of tracks each day, depending on the wind field and the number of aircraft flying, so although westbound tracks are always labelled from A whilst eastbound are labelled in reverse from Z, tracks with the same label on different days are not necessarily similarly efficient. The ATM tracks are used at a variety of different altitudes, but they are optimised at the 250 hPa iso-bar, since, on average, this is where the jet stream is strongest (Mangini *et al* 2018). This pressure level corresponds approximately to Flight Level 340, which is an altitude of 34 000 feet in the International Standard Atmosphere. Mangini *et al* (2018) found that altering altitude between 200 and 300 hPa when flying the ATM tracks, made less than a 1% difference to total route time. Therefore, all simulations in this study have been run at the single pressure altitude of 250 hPa.

Flights from 1 December, 2019 to 29 February, 2020, have been considered as the wind fields in the winter months tend to be at their strongest and most variable. This can be seen when seasonal weather patterns are split into categories; in winter five are used, whereas in summer only three are necessary (Irvine *et al* 2013). This is (at least partly) because transatlantic flight routes in winter vary strongly in response to the North Atlantic Oscillation (Kim *et al* 2016). The average wind speed at typical cruise altitudes in the North Atlantic flight corridor in winter is expected to increase in future, because of climate change, meaning that winds will play an increasingly important role in flight routing (Williams 2016, Simpson 2016, Kim *et al* 2015, 2020).

Past wind field data are obtained from the reanalysis data set provided by the National Center for Atmospheric Research (Kalnay *et al* 1996). Average daily horizontal wind velocities are given every 2.5 degrees of both latitude and longitude, at a range of pressure levels. Given that there is little variation in the wind field at this altitude on timescales of one day (Mangini *et al* 2018), a daily average is sufficiently accurate for these routes. Linear interpolation is used to obtain meridional (northward) and zonal (eastward) winds in between the grid points. Following Lunnon and Mirza (2007) the calculated optimal routes are largely insensitive to the wind grid resolution for journeys of this length, with use of high resolution data making at most a few seconds difference on a transatlantic flight.

Since the flights are long haul, the time and distance covered during climb and descent are small compared to the cruise phase, with flights between LHR and JFK spending about 92% of the ground distance in cruise (Flightradar24 2020). Therefore, we neglect the climb and descent phases in this analysis.

3. Analysis methods

Here methods used to obtain optimised fuel-efficient flight paths are described. The air distance of each route is considered. This is the distance travelled relative to the wind field and so can be calculated by multiplying the time in the air by the airspeed. By contrast, ground distance is the length of the route that the aircraft is observed to have flown from the ground. Thus in a zero wind field, the air distance and the ground distance will be identical and the Great Circle path—the path giving the shortest distance along the ground between two points on a sphere—will be the minimum time route. However, if a wind field is added, then maintaining the Great Circle path (GC path) as the ground track involves a change to the air distance flown, resulting in a flight time that is no longer the minimum.

In this section, the relationship between fuel use and air distance is first established, before the time optimisation method used is outlined.

3.1. Aircraft fuel use

For a given aircraft, the mass of fuel burned per unit time, $\frac{dm_f}{dt}$, depends on the weight of the aircraft, the true airspeed and the altitude (Poll 2018, Poll and Schumann 2020). Hence, if the weight, airspeed and altitude are held constant, as we assume here, the quantity of fuel burned per unit distance travelled through the air, $\frac{dm_f}{ds}$, is also constant. In this case the total fuel required for a journey is the product of $\frac{dm_f}{ds}$ and the total air distance flown, where total air distance is the product of the constant airspeed and the total flight time. Therefore, the total fuel requirement for a flight at a given airspeed is minimised when the total flight time is minimised. Finding the minimum flight time at constant airspeed through a specified wind field is a classical problem in aeronautics, first addressed by Zermelo (1930) and Levi-Civita (1931).

Furthermore, for an aircraft of a given weight at a specified altitude, there is a particular airspeed at which $\frac{dm_f}{ds}$ is also a minimum (Poll 2018, Poll and Schumann 2020). For a modern large, long-range, turbofan-powered aircraft, this optimum airspeed is in the region of 240 m s^{-1} (Mach $\approx$ 0.82). Hence, for a given aircraft travelling between a given airport pair, the absolute minimum fuel requirement is found by calculating the airspeed that minimises the product of $\frac{dm_f}{ds}$ for the aircraft and the minimum air distance through the wind field. Therefore, the complete problem depends on both the aircraft and the wind field. However, since the aircraft-dependent and navigational elements are completely independent, they can be determined separately, before combination for complete analysis.

The work described in this paper addresses the navigational problem of determining the variation of minimum air distance with airspeed for the chosen routes.

3.2. Time optimisation

Time minimisation (and therefore air distance minimisation) is achieved by solving a time optimal control problem, where the dynamics are given by the Zermelo equations on the sphere (Arrow 1949, Bryson and Ho 2010):

$$\frac{d\lambda}{dt} = \frac{u + V\cos\theta}{R\cos\phi} \tag{1}$$

$$\frac{d\phi}{dt} = \frac{v + V\sin\theta}{R} \tag{2}$$

$$\frac{d\theta}{dt} = -\frac{Wind2D}{R\cos\phi} \tag{3}$$

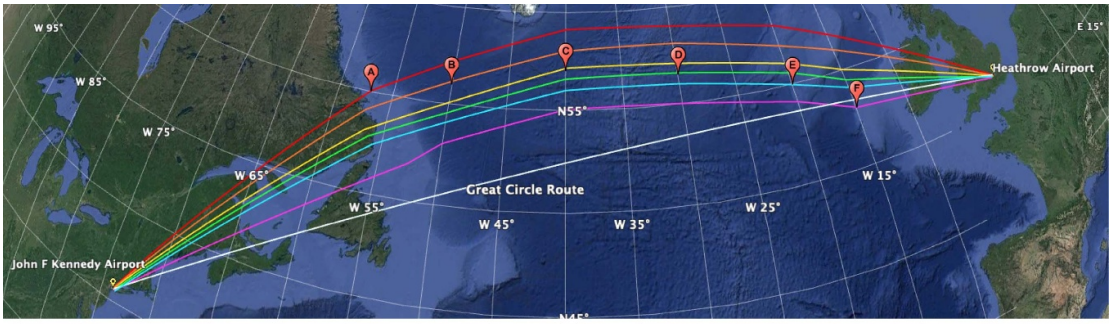

(a) Westbound ATM tracks

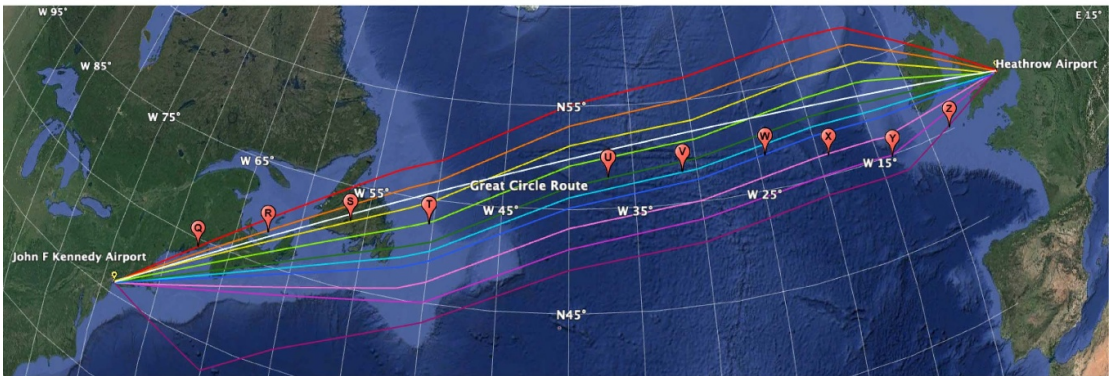

(b) Eastbound ATM tracks

Figure 1. Figure 1(a) shows all westbound tracks between LHR and JFK on the 3 December, 2019. The Great Circle path (GC Path), the shortest distance along the ground between the airports, is shown in white. The six tracks are labelled from A to F and lie predominantly North of the GC path to avoid the prevailing jet stream air currents. They were valid for all flights reaching 30 W from 11:00 to 19:00(UTC). Figure 1(b) shows all eastbound tracks between JFK and LHR on the 3 December, 2019. The GC path is again shown in white. The ten tracks are labelled from Q to Z and lie both sides of the GC path. They were valid for all flights reaching 30 W from 01:00 to 08:00(UTC). Map data: Google, Data SIO, NOAA, U.S. Navy, NGA, GEBCO, Image IBCAO, Image Landsat/Copernicus.

where the *Wind2D* term is:

$$\begin{aligned} Wind2D = &-\sin\theta\cos\theta\frac{\partial u}{\partial\lambda} + u\cos^2\theta\sin\phi \\ &+ \cos^2\theta\cos\phi\frac{\partial u}{\partial\phi} + v\sin\theta\cos\theta\sin\phi \\ &+ \cos\theta\sin\theta\cos\phi\frac{\partial v}{\partial\phi} \\ &+ V\cos\theta\sin\phi - \sin^2\theta\frac{\partial v}{\partial\lambda} \end{aligned} \tag{4}$$

Here t is time from departure, $\lambda(t)$ and $\phi(t)$ are the aircraft's longitude and latitude (radians), $u(\lambda,\phi)$ and $v(\lambda,\phi)$ are zonal and meridional wind speeds (m s^{-1}), R is the radius of the Earth, taken as 6 371 km, V is the constant airspeed (m s^{-1}) and θ is the aircraft's heading angle, the direction in which the nose of the aircraft is pointing, here measured anticlockwise from due east. This is illustrated in figure 3. Initial conditions $\lambda(0)$ and $\phi(0)$ are given by the departure airport's longitude and latitude respectively. The initial value for $\theta(0)$ is unknown and to be determined. Zonal and meridional components of both the wind velocity and the velocity of the aircraft relative to the air are combined to give equations (1) and (2), from which equation (3) is derived, using first-order optimality conditions. (Bryson and Ho 2010, Ng *et al* 2011, 2014).

3.3. Numerical algorithm

We present a numerical method to estimate the unknown initial heading angle $\theta(0)$. Each $\theta(0)$ value will have an associated trajectory, which will be time optimal for this particular set of initial conditions ($\lambda(0), \phi(0)$ and $\theta(0)$), but which will intersect the arrival airport only for certain values of $\theta(0)$. The method we use seeks these values of $\theta(0)$ by locating trajectories which satisfy the optimality system (1)–(3) and also pass within 200 m of the destination airport. These are obtained using extreme initial heading angles of 50 degrees either side of the GC path joining the departure and destination airports. The GC path initial heading from JFK to LHR is 38.7° and from LHR to JFK is 162.1°. Subsequent headings along the route are found by advancing the equations (1)–(3) using the Euler forward step method (Williams 2016). At each aircraft position, the wind field is given by linear interpolation of the reanalysis data. The flight path is calculated by advancing in time in 1 s intervals. The integration duration is taken as 1.8 times the time taken to cover

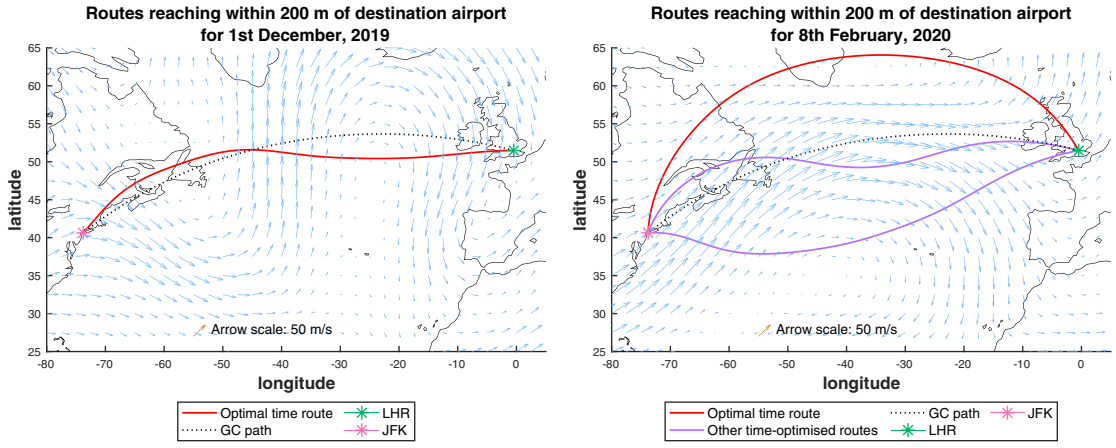

(a) Westbound Quiver Plot 1st December, 2019

(b) Westbound Quiver Plot 8th February, 2020

Figure 2. Quiver plots showing values for wind velocity in m s^{-1} on 1 December 2019 and 8 February, 2020 across the North Atlantic. The westbound time optimal flight paths calculated by numerically integrating equations (1)–(3) for each day's wind field, from LHR to JFK (indicated by green and pink asterisks respectively) are shown in red. The two routes on 8 February 2020 which also reach the airport, but have longer flight times are shown in purple. The GC path is marked as a dotted black line on each plot.

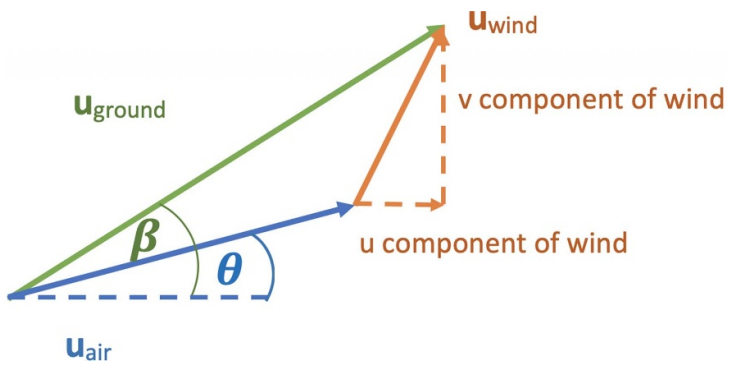

Figure 3. Diagram showing vector triangle of aircraft velocity relative to the ground, $\mathbf{u}_{\text{ground}}$, aircraft velocity relative to the air, $\mathbf{u}_{\text{air}}$, and wind velocity, $\mathbf{u}_{\text{wind}}$. θ is the aircraft's heading angle and β is the rhumb line or ground-track angle, which is the single heading an aircraft in wind-free conditions would take to reach the next waypoint.

the GC path at the chosen airspeed in still air, i.e. when airspeed is equal to ground speed. This duration ensures that, even in the strongest headwinds, the calculated paths will always pass through the destination's meridian.

From the paths for the two extreme initial heading angles, the distance to the destination airport from each point on each route (d) is calculated using the Haversine formula (Veness 2019):

$$a = \sin^2(\Delta lat/2) + \cos(lat1).\cos(lat2).\sin^2(\Delta lon/2) \quad (5)$$

$$c = 2.\text{atan2}(\sqrt{a}, \sqrt{1-a}) \quad (6)$$

$$d = R.c \quad (7)$$

where $lat1$ is the latitude of the first point, $lat2$ is the latitude of the second point, Δlat is the difference in latitudes between the two points, Δlon is the difference in their longitudes and R is the radius of the Earth. The atan2 function is the four-quadrant inverse tangent of the two real values in the function bracket. (The first of these values dictates the y position and the second the x position of a point on Cartesian axes. The returned value is the angle, between $-\pi$ and π, swept out from the positive x-axis to a line joining the origin to the given position.)

If no point within 200 m of the destination airport is found along the two paths, a bisection method is applied to the initial heading angles and the algorithm above is repeated until this criterion is achieved. Minimum time trajectories for airspeeds between 200 and 270 m s^{-1} can be found in this way for all eastbound flights and most westbound flights.

For a small number of westbound flights, the bisection method finds multiple optimal time paths which pass within 200 m of the destination airport, due to routes from more than one initial heading

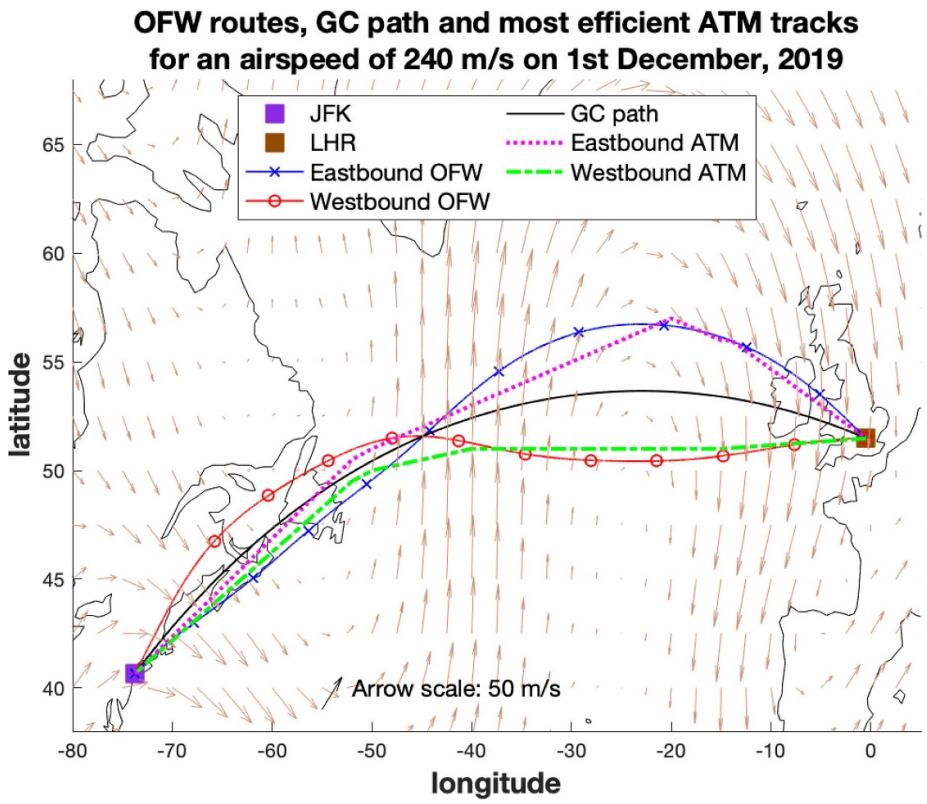

Figure 4. Plots to show the ground tracks of OFW routes and the most efficient ATM tracks flying both east and west between LHR and JFK. The GC path is also shown.

angle fulfilling the success criterion. In these cases the time optimal route with the shortest duration is chosen. For example, paths for 1 December, 2019 and 8 February, 2020 are plotted in figure 2 over a quiver plot showing the wind velocity at each grid point. It can be seen in figure 2 that on 1 December, 2019, the bisection method is successful in finding a single time optimal path. The daily wind field leads to routes with similar initial heading angles changing heading gradually and almost identically, so that they do not cross. In contrast, figure 2 shows that on 8 February, 2020, where the region of stronger adverse wind in the mid-North Atlantic causes flights to change heading more rapidly, three trajectories will reach the destination airport. Only one of these will, however, be a global (within the initial 100° wide search range) minimum time route for the journey, as the flight times differ. For the three time optimal routes shown in figure 2 these flight times are 8 h 53 min for an initial heading angle of 167.5 degrees, 8 h 23 min for an initial heading angle of 196.3 degrees and 7 h 25 min for an initial heading angle of 121.7 degrees.

Thus using the Euler forward method applied to the Zermelo dynamical system, mapped conformally onto a sphere, the minimal time paths can be plotted between airport pairs across a range of air speeds for all 91 days in winter 2019–2020. These paths are called optimised for wind (OFW) routes. From these trajectories the air distance can be found and compared with the air distance of an aircraft with a ground track following the GC path and with the air distances associated with each of the daily ATM tracks in the OTS. Due to the daily wind field data, the air distance for the GC path will not be equal to the GC ground track distance.

3.4. ATM tracks and the GC path

The minimised flight times are used to compute air distances, as a function of airspeed, for all flights between JFK and LHR. Mean time for westbound OFW routes, plus or minus standard deviation, was 415 ± 18.4 min, whilst eastbound it was 323.5 ± 13.7 min. The OFW route air distances are compared with those covered by aircraft following as ground tracks the GC path and the ATM tracks (produced by NAV CANADA and NATS), through the same wind fields. The corresponding air distances for these journeys are calculated as follows.

To validate comparisons between the GC path and the OFW routes, the GC path is split into 25 000 way points. For each pair of consecutive way points, the rhumb line bearing, a single heading that will take an aircraft from the first waypoint to the second around a sphere, is found and the ground speed for each interval calculated by solving the vector equation:

$$\mathbf{u}_{\text{wind}} + \mathbf{u}_{\text{air}} = \mathbf{u}_{\text{ground}} \tag{8}$$

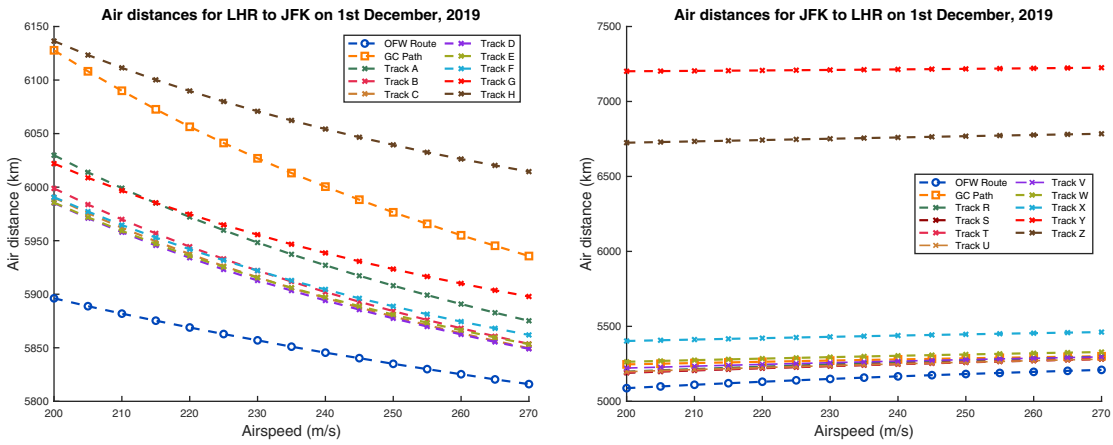

(a) Air distances 1st December, 2019 westbound

(b) Air distances 1st December, 2019 eastbound

Figure 5. The variation of air distance with airspeed for OFW routes, GC paths and ATM Tracks on 1 December, 2019.

where $\mathbf{u}_{\text{wind}}$ is a vector comprised of zonal and meridional wind components, $\mathbf{u}_{\text{air}}$ is a vector giving the aircraft's velocity relative to the air and $\mathbf{u}_{\text{ground}}$ is a vector giving the aircraft's velocity relative to the ground (see figure 3). The sum of the rhumb line distances gives the total ground distance. The rhumb line distances for each interval are divided by the corresponding ground speeds to give the interval times, which are summed to give total flight time. Multiplying the flight time by the airspeed gives the air distance travelled in each case. Air and ground distances for the ATM tracks are calculated in a similar way. The journey between each of the ATM track way points is divided into smaller intervals reflecting the ratio between the length of the journey between these way points and the whole journey distance. Again a total of 25 000 steps is used. Once these intervals are generated, the methods used for the GC path are applied.

4. Results

4.1. Air distance analysis

Air distances for the ATM tracks, GC path and OFW route are now compared. An example of the ground tracks for these paths is given in figure 4. This shows that on the 1 December, 2019, the OFW routes going east are very similar to the most efficient ATM track, but that flying west there is more of a discrepancy. All routes except for the westbound ATM track cross the GC path. The savings in air distance made, can be seen in figure 5, which gives air distances of each route for a range of airspeeds. As expected the OFW route has the shortest air distance for all airspeeds both westbound and eastbound. Air distance reduces as airspeed increases for the westbound tracks, whilst increasing for eastbound flights, since in a strong wind field, airspeed has less effect on air distance when flying with the prevailing wind than against it. As air distance is airspeed multiplied by time, if time is greatly reduced by flying faster, the increase in airspeed does not mean necessarily that air distance is increased. This can be seen in westbound results. Conversely, when aircraft fly east, extra airspeed does not change the time the route takes as dramatically, meaning that the airspeed factor in the air distance product becomes dominant and the air distance increases with airspeed. Both the GC path curves in figure 5 approach the Great Circle ground distance between the two airports (5.6×10^6 m) as the airspeed increases, which is the expected behaviour, because the wind speed becomes less important and so the air distance tends to the ground distance.

The excess air distances that are incurred by flying the ATM tracks and GC path instead of the OFW route, averaged across the whole winter period, are shown in figure 6. Here both westbound and eastbound air distance savings decrease with increasing airspeed, with the exception of savings made when the OFW route is compared with the least efficient eastbound ATM track. In this case the savings increase slightly as airspeed increases, demonstrating that once a track is very far from the advantageous eastbound winds, flying at a higher airspeed will only burn even more fuel and produce even more emissions, without reducing air distance. However, in all other cases, there is slightly less of a saving in air distance as airspeed increases, which means that the ATM tracks require the aircraft to use increased airspeeds to combat less advantageous air currents.

Taking the results for an airspeed of 240 m s^{-1} and averaging savings in air distance between the most efficient ATM track and the OFW route across all 91 days of winter 2019–2020 for flights from JFK to LHR, gives an air distance saving of 37 km, but the saving for the least efficient ATM track is over 931 km. The average saving for all ATM tracks is 232 km. In the opposite direction, flying from LHR to JFK, 54 km of air distance are saved by using the optimised route compared with the most efficient ATM track and air

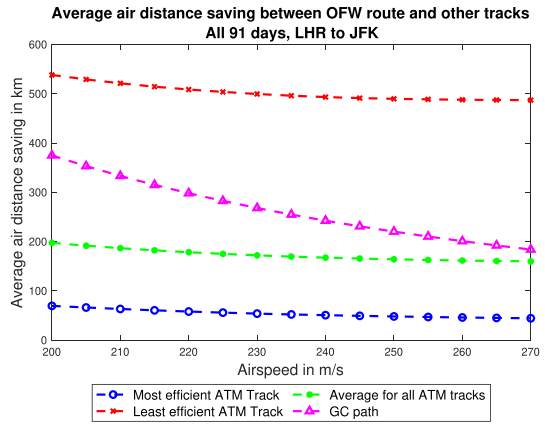

(a) Average air distance westbound

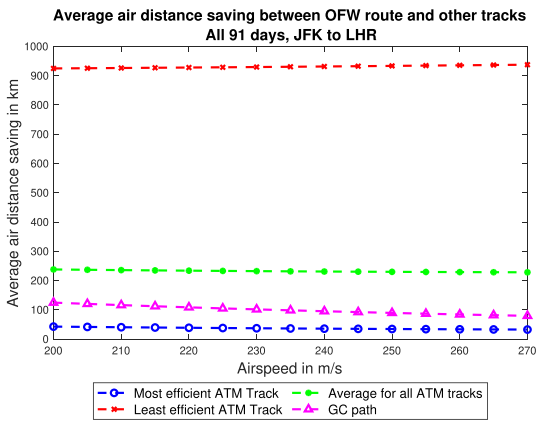

(b) Average air distance eastbound

Figure 6. Plots of air distance saved when the OFW route is compared to the most efficient ATM track, the least efficient ATM track and the average ATM track for each day at each airspeed. Savings compared with the GC path through the same wind field are also shown.

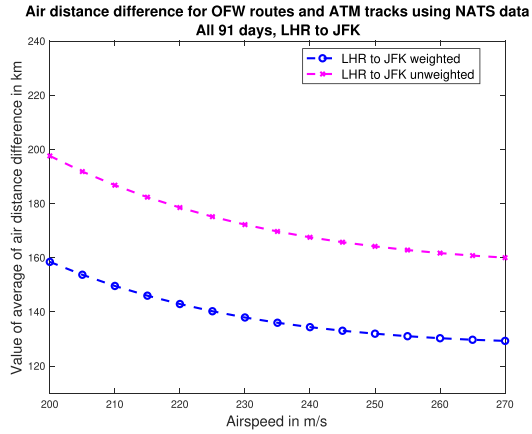

(a) Average air distance difference westbound

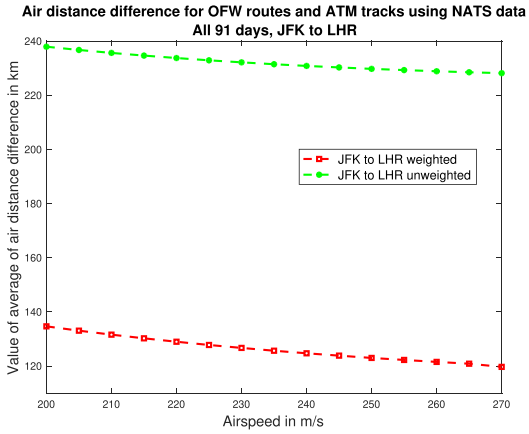

(b) Average air distance difference eastbound

Figure 7. Plots to show the savings to be made on average at each airspeed for aircraft flying both east and west along the route between LHR and JFK. Averages are calculated as if all tracks are used equally for the unweighted results and then as if tracks are used in the same ratio as in the NATS daily track usage figures for all mid-North Atlantic crossings, for the weighted results.

distance is reduced by 502 km compared with the least efficient ATM track. The average across all tracks gives a saving of 173 km. Westbound ATM tracks are normally closer on average to the most efficient track than those going east, explaining the larger eastbound average savings in comparison to each day's least efficient track.

Averaged over all 91 days of data, the difference in air distance between the OFW route and each ATM track is statistically significant at the 95% level using a one-tailed T-test (Student 1908) with unequal variances, for each airspeed. In all cases the adoption of the OFW routes significantly reduces air distance. Percentage improvement in air distance, for flights from JFK to LHR flown at 240 m s^{-1} show a saving of 0.7% when the OFW route is compared to the most efficient ATM tracks, but 16.2% when compared to the least efficient ATM tracks. The average across all tracks gives a saving of 4.7%. For the same journey in reverse the range of savings is from 0.8% to 7.3%, with an average of 2.9%. Table 1 shows all percentage savings across both routes, for a range of airspeeds. Given the large number of flights using these routes every day, adopting the OFW routes would save a significant amount of air distance and thus a significant amount of fuel and greenhouse gas emissions.

4.2. Observed usage of ATM tracks

As shown in the previous section, air distance savings depend to a large extent on the ATM track flown, so track usage statistics are crucial when estimating potential savings. We have obtained such statistics from NATS, giving the number of times each track was flown in each direction each day. A limitation is that all mid-North Atlantic flights are included, not just those between JFK and LHR. Also data for 14 and 15 December, 2019 are not available, so these days have been omitted from the calculations.

Table 1. Table showing percentage savings in air distance for routes in both east and west directions at a range of airspeeds when the OFW route is compared to least (L) and most (M) efficient ATM tracks over the 91 day period between 1 December, 2019 and 29 February, 2020.

Airport		Airspeed in m s^{-1}															
		200		210		220		230		240		250		260		270	
Departure	Destination	M	L	M	L	M	L	M	L	M	L	M	L	M	L	M	L
LHR	JFK	1.08	7.78	0.99	7.59	0.92	7.46	0.85	7.37	0.81	7.32	0.77	7.29	0.74	7.30	0.72	7.31
JFK	LHR	0.90	16.45	0.85	16.37	0.80	16.29	0.77	16.23	0.73	16.18	0.70	16.13	0.68	16.10	0.66	16.06

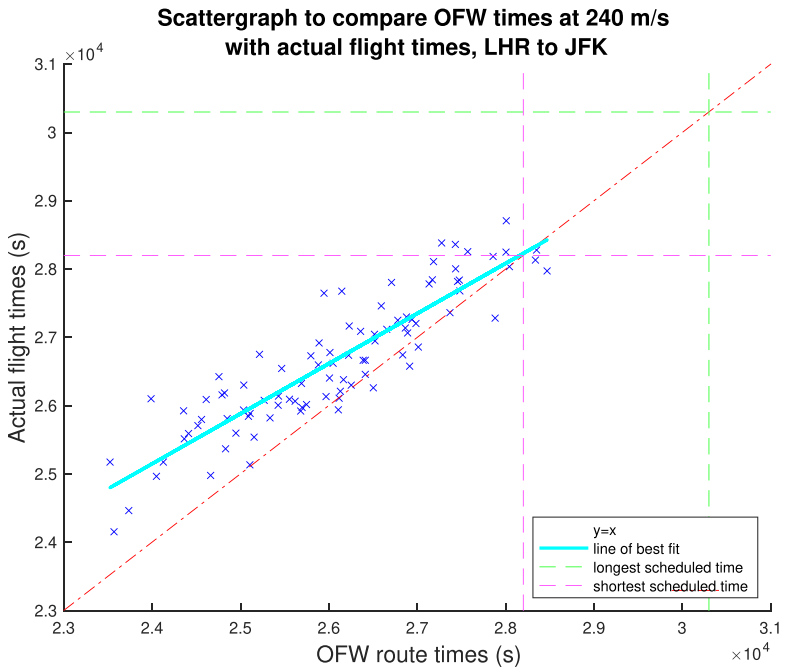

(a) Westbound flights

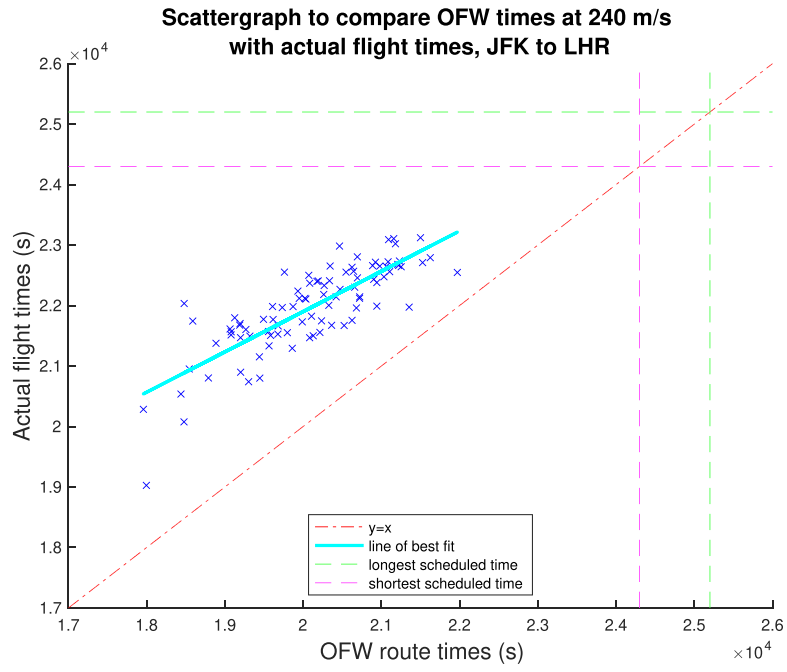

(b) Eastbound flights

Figure 8. Figure 8(a) shows how the optimal westbound times calculated for each day's wind field varied with the average actual flight time recorded each day from JFK to LHR. Figure 8(b) shows the corresponding information for the eastbound route from LHR to JFK.

Nevertheless, using a weighted average, in which tracks are used in the same ratio as in the NATS daily track usage figures, to look at differences in air distance between OFW routes and ATM tracks, provides some insight into potential percentage savings. Figure 7 shows that if airlines use all provided tracks equally their flights are less fuel efficient than the track usage figures from NATS imply. Therefore airlines already have a good idea of where the most fuel and time efficient routes are each day. The percentage saving obtained, using this weighted average for flights at a constant airspeed of 240 m s^{-1}, is 2.5% for eastbound flights and 1.7% for those flying west. Thus with more flexibility allowed in the track system, fuel savings could be made, enabling a significant reduction in emissions.

4.3. Limitations

The limitations of the current approach lie in the simplification of the underlying model. Aiming for the minimum time for a route does not necessarily fit the reality of a timetable of scheduled flights. However, other assumptions such as maintaining the same altitudes and airspeeds for the cruise phase could be adjusted in future work to allow flight times to be fixed. This would allow aircraft to benefit from different wind fields at different altitudes. In figure 8 average actual flight times from LHR to JFK are compared with those found by time optimisation across each daily wind field, for all flights made from 1 December, 2019 to 29 February, 2020. The actual flights have varying airspeeds, with cruising airspeeds of between 230 and 250 m s^{-1}. As the actual flights are not entirely in cruise phase and are not optimised for time, most actual flight times are longer than the OFW route times, as is shown by the data points lying above the red line. However, on a handful of days the opposite is true, as flights are not constrained to a single airspeed or altitude. The green and pink lines on the plot show the shortest and longest scheduled times for a crossing from LHR to JFK. Data being widely spread from these boundaries, reveal that current scheduling includes much taxiing and contingency time, timetables being written long before airlines know the nature of the daily wind fields. However, during this period, 11 westbound flights did exceed their scheduled time, presumably due to exceptionally strong winds.

In figure 8 the same patterns are shown for the journey from JFK to LHR. In this case, all flights have shorter OFW route times. All eastbound flights during the 2019–2020 winter period landed well within their scheduled times.

Both OFW route times and average actual times are found to be normally distributed in a single-sample Kolmogorov–Smirnov test, at a 95% level of significance, so a product moment correlation coefficient can be calculated. This shows that there is a strong positive correlation between datasets, as shown by the turquoise line of best fit in figure 8. The shallow gradient of this line, which is less than one for both eastbound and westbound flights, shows that as flights take longer, the difference between the actual flight times and the optimised flight times becomes smaller, as taxi, take-off and landing phases take a set time and so for longer flights they become a smaller percentage of the whole trip. The line of best fit for the westbound journeys is steeper than that for the eastbound journeys, as the OFW routes save more air distance in this direction.

5. Summary and conclusions

Using wind-optimised tracks would reduce North Atlantic air distances significantly, even in comparison to the most efficient current ATM tracks. At present, the ATM tracks are heavily constrained by safety considerations driven by the poor situational awareness available over the mid-Atlantic. This results in a track system that is sub-optimal for fuel use and thus airlines are obliged to produce excess emissions. Airlines also currently choose routes that minimise the total cost of operating a flight (by specifying a Cost Index, which is the ratio of time-related costs to fuel costs), not the fuel consumption or emissions. With more reliable and high-resolution situational awareness available, greater track flexibility should be possible enabling worthwhile fuel savings to be made by the airlines and reducing emissions. This work demonstrates a way to compare the current North Atlantic ATM Tracks with routes generated by a time optimisation method based on solutions of the spherical version of the Zermelo equations. Air distance is used as a measure of the efficiency of ATM tracks. Savings of between 0.7% and 16.4% in air distance can be made by adopting time-optimised routes through each daily wind field, with level of savings dependent on flight direction and chosen ATM track.

To estimate the potential CO_2 emissions savings over a whole winter period, consider the 3 833 701 seats provided between New York and London in 2019 (OAG 2020). According to the ICAO carbon emissions calculator (2020), an economy class return flight between London and New York generates 670 kg of CO_2 per passenger. Taking an airspeed of 240 m s^{-1}, an average saving of 1.7% can be assumed for the 479 333 passengers flying west over the winter period and an average saving of 2.5% can be assumed for the 479 093 passengers flying east. These figures are derived from the weighted averages for the air distance savings as discussed in section 4.2 and from assuming that one quarter of the annual flight figures provided by OAG (OAG 2020) pertain to winter flights. This gives a potential saving of over 6.7 million kg of CO_2 emissions across the winter period of each year alone.

Here we investigated optimal flight trajectories given a deterministic wind field. In future studies we plan to investigate the design of optimal routes that are robust under uncertain weather conditions. It would also be useful for airlines to be able to have the flexibility to change horizontal route, altitude and airspeed in order to make flight times more uniform, whilst also keeping fuel burn and thus emissions to a minimum. This will be a priority for future research.

Data availability statement

The data that support the findings of this study are available upon reasonable request from the authors.

Acknowledgment

CAW is supported by the Mathematics of Planet Earth Centre for Doctoral Training at the University

of Reading. This work has been made possible by the financial support of the Engineering and Physical Sciences Research Council, Grant Number EP/L016613/1. DK's involvement in this research benefited from the support of the FMJH 'Program Gaspard Monge for optimization and operations research and their interactions with data science', and from the support from EDF, Thales and Orange. NKN is supported in part by the NERC National Centre for Earth Observation (NCEO). We would like to thank Mr Ian Jopson from NATS for the provided ATM track usage data.

ORCID iDs

Cathie A Wells https://orcid.org/0000-0001-9438-4954
Paul D Williams https://orcid.org/0000-0002-9713-9820
Nancy K Nichols https://orcid.org/0000-0003-1133-5220
Dante Kalise https://orcid.org/0000-0003-2327-1957
Ian Poll https://orcid.org/0000-0001-8057-8467

References

Aireon 2020 Operations overview (available at: https://aireon.com/resources/overview-materials/operations-overview/)
Arrow K 1949 On the use of winds in flight planning *J. Meteorol.* **6** 150–9
Burrows J W 1983 Fuel-optimal aircraft trajectories with fixed arrival times *J. Guid. Control Dyn.* **6** 14–9
CAPA 2018 Record global aircraft deliveries in 2017: Boeing ahead of Airbus again, but behind on order backlog January (available at: https://centreforaviation.com/analysis/reports/record-global-aircraft-deliveries-in-2017-boeing-ahead-of-airbus-again-but-behind-on-order-backlog-393914)
Cheung J C H 2018 Flight planning: node-based trajectory prediction and turbulence avoidance *Meteorol. Appl.* **25** 78–85
Coffel E and Horton R 2015 Climate change and the impact of extreme temperatures on aviation *Weather Clim. Soc.* **7** 94–102
Dhief I 2018 Optimization of aircraft trajectories over the North Atlantic Airspace *PhD Thesis* Université Paul Sabatier
Flightradar24 A 2020 Flight data (https://www.flightradar24.com/data/flights)
Franco A and Rivas D 2011 Minimum-cost cruise at constant altitude of commercial aircraft including wind effects *J. Guid. Control Dyn.* **34** 1253–60
Gratton G, Padhra A, Rapsomanikis S and Williams P D 2020 The impacts of climate change on Greek airports *Clim. Change* **160** 219–31
Graver B, Zhang K and Rutherford D 2019 CO_2 emissions from commercial aviation, 2018 *Working Paper 2019-16* 16 (ICCT) 13 (https://theicct.org/sites/default/files/publications/ICCT_CO2-commercl-aviation-2018_20190918.pdf)
Green J E 2009 The potential for reducing the impact of aviation on climate *Techn. Anal. Strat. Manag.* **21** 39–59
Grewe V *et al* 2017 Feasibility of climate-optimized air traffic routing for trans-atlantic flights *Environ. Res. Lett.* **12** 034003
Grewe V, Matthes S and Dahlmann K 2019 The contribution of aviation NOx emissions to climate change: are we ignoring methodological flaws? *Environ. Res. Lett.* **14** 121003
Grobler C *et al* 2019 Marginal climate and air quality costs of aviation emissions *Environ. Res. Lett.* **14** 114031
Henderson R, Martins J and Perez R 2012 Aircraft conceptual design for optimal environmental performance *Aeronaut. J.* **116** 1–22
ICAO 2016 *On Board: A Sustainable Future 2016 Environmental Report* (https://www.icao.int/environmental-protection/Pages/env2016.aspx)
ICAO 2019 Destination green: the next chapter (https://www.icao.int/environmental-protection/Documents/EnvironmentalReports/2019/ENVReport2019_pg111-115.pdf)
ICAO 2020 Carbon emissions calculator (https://www.icao.int/environmental-protection/Carbonoffset/Pages/default.aspx)
IPCC 2019 Special Report on the Ocean and Cryosphere in a Changing Climate (https://www.ipcc.ch/srocc)
Irvine E, Hoskins B, Shine K, Lunnon R and Froemming C 2013 Characterizing North Atlantic weather patterns for climate-optimal aircraft routing *Meteorol Appl.* **20** 80–93
Irvine E, Shine K and Stringer M 2016 What are the implications of climate change for trans-atlantic aircraft routing and flight time? *Transp. Res.* D **47** 44–53
Jardin M and Bryson A 2010 Methods for Computing Minimum-Time Paths in Strong Winds *Journal of Guidance, Control and Dynamics* **35** 165–71
Jardin M and Bryson A 2012 Neighboring optimal aircraft guidance in winds *18th Applied Aerodynamics Conf* (https://doi.org/10.2514/6.2000-4264)
Jensen L, Tran H and Hansman R 2015 Cruise fuel reduction potential from altitude and speed optimization in global airline operations *USA/Europe Air Traffic Management Research and Development(ATM) Seminar* **141** 764–73
Kalnay E *et al* 1996 The NCEP/NCAR 40-year reanalysis project *Bull. Am. Meteorol. Soc.* **77** 437–72
Karnauskas K B, Donnelly J P, Barkley H C and Martin J E 2015 Coupling between air travel and climate *Nat. Clim. Change* **5** 1068–73
Kim J-H, Chan W N, Sridhar B, Sharman R D, Williams P D and Strahan M 2016 Impact of the North Atlantic oscillation on transatlantic flight routes and clear-air turbulence *J. Appl. Meteorol. Climatol.* **55** 763–71
Kim J-H, Chan W, Sridhar B and Sharman R 2015 Combined winds and turbulence prediction system for automated air-traffic management applications *Appl. Meteor. Climatol* **54** 766–84
Kim J-H, Kim D, Lee D, Chun H, Sharman R, Williams P D and Kim Y 2020 Impact of climate variabilities on trans-oceanic flight times and emissions during strong NAO and ENSO phases *Environ. Res. Lett.* **15** 105017
Lee D *et al* 2020 The contribution of global aviation to anthropogenic climate forcing for 2000 to 2018 *Atmos. Environ.* **244** 117834
Lee S H, Williams P D and Frame T H A 2019 Increased shear in the North Atlantic upper-level jet stream over the past four decades *Nature* **572** 639–42
Levi-Civita T 1931 über Zermelo's Luftfahrtproblem *ZAMM - J. Appl. Math. Mech. / Zeitschrift für Angewandte Mathematik und Mechanik* **11** 314–22
Lunnon R and Mirza A 2007 Benefits of promulgating higher resolution wind data for airline route planning *Meteorol. Appl.* **14** 253–61
Mangini F, Irvine E, Shine K and Stringer M 2018 The dependence of minimum-time routes over the North Atlantic on cruise altitude *Meteorol. Appl.* **25** 655–64
Monbiot G 2006 *Heat: How We Can Stop the Planet Burning* (London: Allen Lane)

Murrieta Mendoza A, Romain C and Botez R 2020 3D Cruise trajectory optimization inspired by a shortest path algorithm *Aerospace* **7** 99

NATS 2019 Aireon system goes live–trial operations begin over the North Atlantic marking new chapter in aviation history (https://www.nats.aero/news/aireon-system-goes-live/)

Németh H, Ṣvec M and Kandráç P 2018 The influence of global climate change on the European Aviation *Int. J. Eng. Appl. (IREA)* **6** 179–86

Ng H K, Sridhar B and Grabbe S 2014 Optimizing aircraft trajectories with multiple cruise altitudes in the presence of winds *J. Aerosp. Inf. Sys.* **11** 35–47

Ng H K, Sridhar B, Grabbe S and Chen N Y 2011 Cross-polar aircraft trajectory optimization and the potential climate impact *2011 IEEE/AIAA 30th Digital Avionics Conf.* pp 1–19

OAG 2020 Busiest routes 2019 (https://www.oag.com/reports/busiest-routes-2019)

Pierson B L and Ong S 1989 Minimum-fuel aircraft transition trajectories *Math. Comput. Modelling* **12** 925–34

Poll D I A 2018 On the relationship between non-optimum operations and fuel requirement for large civil transport aircraft, with reference to environmental impact and contrail avoidance strategy *Aeronaut. J.* **122** 1827–70

Poll D and Schumann U 2020 An estimation method for the fuel burn and other performance characteristics of civil transport aircraft in the cruise. Part 1 fundamental quantities and governing relations for a general atmosphere *Aeronaut. J.* 1–39

Ryley T, Baumeister S and Coulter L 2020 Climate change influences on aviation: a literature review *Transp. Policy* **92** 55–64

Simpson I 2016 Climate change predicted to lengthen transatlantic travel times *Environ. Res. Lett.* **11** 031002

Storer L N, Williams P D and Joshi M M 2017 Global response of clear-air turbulence to climate change *Geophys. Res. Lett.* **44** 9976–84

Student B 1908 The probable error of a mean *Biometrika* **6** 1–25

Teoh R, Schumann U, Majumdar A and Stettler M 2020 Mitigating the climate forcing of aircraft contrails by small-scale diversions and technology adoption *Environ. Sci. Technol.* **54** 2941–50

Timperley J 2019 Corsia: The UN's plan to 'offset' growth in aviation emissions after 2020 (https://www.carbonbrief.org/corsia-un-plan-to-offset-growth-in-aviation-emissions-after-2020)

Veness C 2019 Calculate distance, bearing and more between latitude/longitude points (https://www.movable-type.co.uk/scripts/latlong.html)

Williams P D 2016 Transatlantic flight times and climate change *Environ. Res. Lett.* **11** 024008

Williams P D 2017 Increased light, moderate and severe clear-air turbulence in response to climate change *Adv. Atmos. Sci.* **34** 576–86

Williams P D and Joshi M 2013 Intensification of winter transatlantic aviation turbulence in response to climate change *Nat. Clim. Change* **3** 644–8

Zermelo E 1930 über die Navigationin der Luft als Problem der Variationsrechnung *Jahresbericht der Deutschen Mathematiker-Vereinigung* **39** 44–8